IEEE Access
Multidisciplinary | Rapid Review | Open Access Journal

Received November 29, 2017, accepted December 30, 2017, date of publication January 18, 2018,
date of current version March 12, 2018.

Digital Object Identifier 10.1109/ACCESS.2018.2794959

Estimation of Modulation Index for Partial Response CPM Signal

TAYYABA MUNAWAR, SAJID SALEEM, (Member, IEEE), SYED ALI HASSAN, (Senior Member, IEEE), AND SYED MOHAMMAD HASSAN ZAIDI

School of Electrical Engineering and Computer Science, National University of Sciences and Technology, Islamabad 44000, Pakistan

Corresponding author: Syed Ali Hassan (ali.hassan@seecs.edu.pk)

ABSTRACT Continuous phase modulation (CPM) is a power and bandwidth efficient modulation scheme used in cellular, personal, and satellite communications among other applications. If the modulation index of the CPM waveform used by the transmitter is unavailable at the receiver, serious performance degradation may occur. This paper investigates the problem of modulation index estimation for partial response continuous phase modulation schemes. Specifically, we propose two novel estimators for the CPM signal observed in an additive white Gaussian noise channel. A non-data aided method of moments (MoM) estimator based upon the fourth-order cumulants and a data-aided best linear unbiased estimator (BLUE) based upon an approximate linear phase model of the received CPM signal have been proposed. Modified Cramer–Rao lower bound is derived for the partial response CPM schemes to assess the performance of the estimators. We also perform numerical simulations to compare the mean-squared error (MSE) performance of the proposed MoM and BLUE estimators with previously proposed estimators in the literature. It is shown that the MoM estimator exhibits good MSE performance at low signal-to-noise ratio (SNR) while the BLUE estimator performs very well at high SNRs. Moreover, the proposed estimators have lower complexity than existing methods and are based upon non-iterative algorithms.

INDEX TERMS Estimation, Cramer-Rao bounds, continuous phase modulation, partial response signaling.

I. INTRODUCTION

Continuous phase modulation (CPM) combines attributes of continuous phase and constant envelope [1], [2]; properties desirable for efficient wireless systems. Phase continuity makes the system spectrally efficient whereas constant envelope provides a power efficient transmission. These characteristics make the CPM scheme popular for various cellular as well as personal communication systems, such as global system for mobile (GSM) [3], digital enhanced cordless telecommunication (DECT) [4], Bluetooth [5], AIS [6], etc. CPM waveforms are either full response or partial response depending upon whether the phase changes corresponding to a transmitted signal are introduced by the transmitter in one symbol interval or they span multiple symbol intervals, respectively. The phase change is gradual for the partial response CPM waveforms and may last up to eight symbol intervals (for example, the shaped-offset quadrature phase shift keying (SOQPSK-TG) waveform used in the aeronautical telemetry IRIG-106 standard). The gradual phase change results in a compact spectrum for the partial response modulation schemes. This bandwidth efficiency is, however, attained at a cost, i.e., the increased receiver complexity due to the additional memory introduced in the transmitted waveform. One of the key parameters that define a CPM signal is its modulation index that controls the phase sensitivity with respect to the input symbols. A CPM waveform with larger modulation index has generally better minimum distance properties and consequently exhibits better performance.

The accurate value of modulation index must be known at the receiver for reliable detection of the signal. However, the knowledge of modulation index may be missing at the receiver because of the variations in the transmitted signal. The modulation index may be unavailable at the receiver either due to an unreliable component or due to the lack of cooperation between the transmitter and the receiver. Modulation index depends on the gain of voltage-controlled oscillator (VCO), which may not be well calibrated or may exhibit uncontrolled variations. In many communication standards such as Bluetooth BR [5], DECT-ULE [4], AIS [6], etc., the modulation index can take values in a certain interval to allow for the tolerance around the nominal modulation index value. For example, for AIS standard, the modulation index

used at the transmitter may belong to the interval [0.35, 0.70]. The tolerance is allowed to enable low cost implementations of the transceivers, which is crucial to the wide adoption and acceptability of a communications standard. On the other hand, for the ideal maximum-likelihood sequence detector (MLSD) and other sub-optimal detectors [7], significant performance degradation is observed [8]. Basic transceiver implementations use the nominal value of modulation index to build the receiver. Although this strategy results in a simple transceiver, but the mismatch present between the modulation index values used at the transmitter and receiver seriously affects the overall system performance. This mismatch could be large in case of non-cooperative transmission or for a system using adaptive modulation schemes.

There are three ways to address the problem of modulation index mismatch at the receiver. The first strategy is to employ a receiver that is robust to the minor mismatch in the modulation index. One such scheme has been recently proposed that is based upon the principal pulse of the Laurent decomposition of the signal [9]. The receiver is very robust to small mismatches in the value of the modulation index but bit-error-rate (BER) performance eventually deteriorates if the modulation index mismatch is of modest magnitude (greater than 0.05). Moreover, the robustness may also reduce for partial response and non-binary schemes, which have more than one principal pulse [10]. The second approach to solve the mismatch issue is to develop CPM waveforms whose performance is relatively insensitive to the modulation index mismatch. A binary CPM scheme that uses ternary pre-coders has been proposed, which achieves robustness at the expense of either increased receiver complexity or undesirable spectral properties [8]. Finally, the performance at the receiver can be improved by estimating the modulation index at the receiver prior to detection. These existing estimators are discussed in the sequel.

Many works have been devoted earlier for the problem of the estimation of modulation index for various CPM schemes [11]–[15]. For example, [11] considers the design of a non-data aided estimator for binary full response CPM schemes which uses higher order statistics (HOS) of the received signal. The estimator achieves good performance at low signal-to-noise ratio (SNR) but it is applicable only to the binary full response CPM signals with rectangular phase shaping functions. Another non-data aided estimator (NDA-CYC) is proposed in [12], which uses the cyclo-stationary properties of the CPM signals [16]. The NDA-CYC is a an iterative estimator that has also been extended to the scenario of joint estimation of miscellaneous parameters of the CPM waveform [13]. The performance of estimator is limited at low SNR owing to phase unwrapping errors. In [14], a data-aided algorithm (DA-LNDIF) is proposed based on Laurents decomposition to perform the modulation index estimation for binary CPM signals [17]. The DA-LNDIF algorithm uses the outputs of the matched filter formed by the principal Laurent pulse. The outputs of the matched filter are equalized to limit the overall memory of CPM to two symbol intervals. The resulting estimator achieves very good performance at low SNR but the performance does not improve considerably at high SNR. Also, the performance degrades when partial response memory is increased. The estimator proposed in [15] considers a finite number of possible hypotheses for the modulation index values and selects the one that maximizes the likelihood function. The performance and complexity of this estimator are dependent upon the cardinality of the set of hypotheses.

The existing algorithms are not readily applicable to the partial response modulation schemes that are mostly used in the standards, e.g., Bluetooth [5], DECT-ULE [4] and SOQPSK-TG [18] waveform used in aeronautical telemetry. The objective of this work is to consider the problem of modulation index estimation for partial response CPM signals. In this paper, we derive two novel estimators for partial response CPM signals observed in additive white Gaussian noise (AWGN). The first proposed approach is a method of moments (MoM) estimator that is based on higher order statistics of the signal, specifically, a ratio of fourth-order cumulants. The MoM estimator shows superior performance at low SNR as compared to the NDA-CYC estimator [12]. Moreover, it is non-iterative and has lower computational complexity than NDA-CYC. The second proposed estimator is a data-aided best linear unbiased estimator (BLUE) based on an approximate linear phase model [19], [20]. The linear phase model was originally developed for estimating the frequency of a sinusoid observed in white Gaussian noise. Here, this frequency estimation algorithm has been employed to estimate the modulation index of both binary and non-binary partial response CPM waveforms with arbitrary phase shaping functions. A comparison of the mean-squared error (MSE) of our proposed linear estimator with that of DA-LNDIF [14] shows that our estimator outperforms at high SNR and approaches the linear performance bound. Moreover, the performance of the BLUE estimator is incredibly robust to increasing partial response memory. Another significant contribution of this work is the derivation of the modified Cramer-Rao lower bound (MCRLB) for this estimation problem. The MCRLB serves as a performance benchmark for the proposed estimators. The expression of MCRLB is applicable to both binary/non-binary and full/partial response CPM schemes of arbitrary phase shaping functions.

In the sequel, we describe the CPM signal model followed by the derivation of the proposed estimators in Sect. III. The MCRLB of modulation index is derived in Sect. IV. Simulation results are presented in Sect. V followed by conclusions in Sect. VI.

II. CPM SIGNAL MODEL

The complex envelope of a CPM signal can be represented as

$$s(t) = Ae^{j\phi(t,\alpha)}, \tag{1}$$

where A is the signal amplitude and $\phi(t, \alpha)$ is the excess phase given by

$$\phi(t, \alpha) = 2\pi h \sum_{i=-\infty}^{m} \alpha_i q(t - iT), \quad \text{for } t \leq mT. \tag{2}$$

Here $\alpha_i \in \{\pm 1, \pm 3, \ldots, \pm(M-1)\}$ form a sequence α of M-ary information symbols. For binary modulation schemes, i.e., for $M = 2$, $\alpha_i \in \{+1, -1\}$. Moreover, the symbols α_i are assumed to be equally likely and memoryless. In (2), the modulation index is denoted by h, whereas, T is the symbol period. The function $q(t)$ is the phase shaping function which is defined as the integral of the underlying frequency shaping pulse $g(t)$. The frequency shaping function $g(t)$ is non-zero over the interval $t \in [0, LT]$ and 0 outside the interval, where L is the partial response length. If the support of $g(t)$ is equal to one symbol interval, i.e., $L = 1$, the signal is called full-response CPM and if the support of $g(t)$ is greater than one symbol interval, the signal is called partial-response CPM.

The CPM signal $s(t, \alpha)$ (1) can be uniformly sampled to get

$$s[n] := s(t)|_{t=nT_s} = Ae^{j\phi[n,\alpha]}, \tag{3}$$

where T_s is the sampling interval expressed as $T_s = T/N_s$ and N_s denotes the number of samples per symbol. Similarly, the excess phase can be discretized as

$$\phi\,[n, \alpha] := \phi\,(n, \alpha)\,|_{t=nT_s} = 2\pi h \sum_{i=-\infty}^{m} \alpha_i q_{n-iN_s}, \tag{4}$$

where n is the sample index, $i = \lfloor \frac{n}{N_s} \rfloor$ is the symbol index, N be the number of available symbols, and $q_n := q(t)|_{t=nN_s}$. The operator $\lfloor(.)\rfloor$ is the floor operator.

The transmitted signal is passed through an AWGN channel such that the received signal (after appropriate pre-filtering and sampling at the receiver) can be approximately expressed as

$$r\,[n] = s\,[n] + w\,[n]\,, \tag{5}$$

where $w[n]$ is the white Gaussian noise with variance σ^2. Note that without proper pre-filtering, the noise will have infinite variance.

III. PROPOSED ESTIMATORS

In this work, we propose two novel estimators for the modulation index estimation of partial response CPM signals. The first estimator is a non-data aided estimator based on the method of moments (MoM) technique [21] applicable to binary CPM signals with rectangular phase shaping functions. It uses the 4-th order cumulant of the received CPM signal. The second estimator is a data-aided best linear unbiased estimator (BLUE), which considers the differential phase of the received signal and is more generally applicable to non-binary CPM and all phase shaping functions. In the sequel, we derive the closed-form expressions of the proposed estimators.

A. METHOD OF MOMENTS ESTIMATOR

The estimator proposed in this section is inspired from the work of [11], which proposes a method for the estimation of modulation index of full response CPM using higher-order statistics, specifically, the auto-correlation and fourth-order cumulants. However, the algorithm had not been developed for the partial response CPM signals, which are more common in modern aeronautical telemetry and wireless personal area networks. It has also been shown [12] that the direct application of the full-response estimation algorithm in [11] to partial response signals results in very poor performance. Hence, a new solution for the problem is required.

The proposed MoM estimator is derived based on the moments of the CPM signal sampled at the symbol rate, i.e., for this section, we assume $N_s = 1$. The autocorrelation function for a full-response CPM signal can be expressed as

$$R_f[m] = \mathbb{E}\{s^*[n]s[n+m]\} = A^2 cos(\pi h)^{|m|}, \tag{6}$$

where $\mathbb{E}$ denotes the expectation operator. Similarly, the fourth-order cumulant [22] is defined as

$$\begin{aligned} &c(m_1, m_2, m_3) \\ &\quad = \mathbb{E}\{s^*[n]s[n+m_1]s[n+m_2]s^*[n+m_3]\} \\ &\qquad - \mathbb{E}\{s^*[n]s[n+m_1]\}\mathbb{E}\{s[n+m_2]s^*[n+m_3]\} \\ &\qquad - \mathbb{E}\{s^*[n]s[n+m_2]\}\mathbb{E}\{s[n+m_1]s^*[n+m_3]\} \\ &\qquad - \mathbb{E}\{s^*[n]s^*[n+m_3]\}\mathbb{E}\{s[n+m_1]s[n+m_2]\}, \end{aligned} \tag{7}$$

which can be expressed as

$$c_f(0, 0, m) = -A^4 cos(\pi h)^{|m|}, \tag{8}$$

for the full response binary CPM signal using the auto-correlation function in (6) [11]. Similarly, the auto-correlation and fourth-order cumulant function for the partial response binary CPM can be derived by using a series of steps as given below.

Using (3) and (4), the sampled signal for $N_s = 1$ can be expressed as

$$s[n] = Ae^{j2\pi h \sum_{i=-\infty}^{n} \alpha_i q_{n-i}}. \tag{9}$$

For a CPM signal with partial response length L, an alternate way to express $s[n]$ is to factorize the cumulative phase and correlative phase components of the signal, i.e.,

$$s[n] = Ae^{j\pi h \sum_{i=-\infty}^{n-L} \alpha_i} e^{j2\pi h \sum_{i=0}^{L-1} \alpha_{n-i} q_i}, \tag{10}$$

where we have used the fact that $q_i = \frac{1}{2}$ for $i \geq L$. Now evaluating the CPM signal at unit lag, we obtain

$$s[n+1] = Ae^{j\pi h \sum_{i=-\infty}^{n-L+1} \alpha_i} . e^{j2\pi h \sum_{i=0}^{L-1} \alpha_{n-i+1} q_i}, \tag{11}$$

which after a change of variable becomes

$$s[n+1] = Ae^{j\pi h \sum_{i=-\infty}^{n-L} \alpha_i} e^{j2\pi h \sum_{i=0}^{L-1} \alpha_{n-i} q_{i+1}}, \tag{12}$$

since $q_0 = 0$ and $q_L = \frac{1}{2}$. Now, the autocorrelation function for partial response CPM is defined as

$$R[m] = \mathbb{E}\{s^*\,[n]\,s\,[n+m]\}, \tag{13}$$

where m is the time lag. It is clear that $R[0] = A^2$. Evaluating (13) at $m = 1$, we get

$$R[1] = \mathbb{E}\{Ae^{-j\pi h\sum_{i=-\infty}^{n-L}\alpha_i}.e^{-j2\pi h\sum_{i=0}^{L-1}\alpha_{n-i}q_i} \times Ae^{j\pi h\sum_{i=-\infty}^{n+1-L}\alpha_i}.e^{j2\pi h\sum_{i=0}^{L-1}\alpha_{n+1-i}q_i}\}, \quad (14)$$

which can be reduced to

$$R[1] = A^2\mathbb{E}\{e^{j2\pi h\sum_{i=0}^{L-1}\alpha_{n-i}(q_{i+1}-q_i)}\}. \quad (15)$$

Using the independence of symbols α_i, we can write the autocorrelation as

$$R[1] = A^2\prod_{i=0}^{L-1}\mathbb{E}\{e^{j2\pi h\alpha_{n-i}(q_{i+1}-q_i)}\}. \quad (16)$$

Since α_i is uniformly distributed over $\{\pm 1\}$, using Euler's identity, we obtain

$$R[1] = A^2\prod_{i=0}^{L-1}cos\left[2\pi h\left(q_{i+1}-q_i\right)\right]. \quad (17)$$

For rectangular phase shaping functions,

$$q_i = q(t)|_{t=iT} = \frac{i}{2L}, \quad \text{for } 0 \le i \le L, \quad (18)$$

which can be used to express (17) in a compact form as

$$R[1] = A^2cos^L\left(\frac{\pi h}{L}\right). \quad (19)$$

Using the expression for the auto-correlation, we can compute some values of the fourth-order cumulant (see (7)) for partial response modulation scheme, i.e.,

$$c(0,0,0) = -A^4 \quad (20)$$

and

$$c(0,0,1) = -A^4cos^L\left(\frac{\pi h}{L}\right), \quad (21)$$

where the last term in (7) is zero owing to the expectation being zero over the cumulative phase values, i.e., $\mathbb{E}\{e^{j2\pi h\sum_{i=-\infty}^{n-L}\alpha_i}\} = 0$. For detailed derivation of (20) and (21), see Appendix. A ratio of these cumulants in (20) and (21) can be expressed as a function of h as

$$c_3 = \frac{c(0,0,1)}{c(0,0,0)} = \cos^L\left(\frac{\pi h}{L}\right). \quad (22)$$

A method of moments estimator for modulation index of partial response CPM with rectangular phase shaping function could now be designed using this ratio of cumulants function as in [11], i.e.,

$$\hat{h}_{MoM} = \frac{L}{\pi}\cos^{-1}\left(\sqrt[L]{\frac{\hat{c}(0,0,1)}{\hat{c}(0,0,0)}}\right), \quad (23)$$

where $\hat{c}(0,0,0)$ and $\hat{c}(0,0,1)$ are the consistent estimators for $c(0,0,0)$ and $c(0,0,1)$, respectively. It should be noted that the estimator is more generally applicable to all binary CPM signals with separable phase shaping functions [23].

B. LINEAR ESTIMATOR

In order to derive a linear estimator, we use the approximate model proposed in [19] and [20] for the estimation of frequency of a sinusoid in noise. This model uses the differential phase of the received signal and is based on the assumption that at high SNR, the received signal can be approximated as

$$r[n] \approx Ae^{j(\phi[n,\alpha]+u[n])}, \quad \text{for } n = 0, 1, \ldots, NN_s - 1. \quad (24)$$

where $u[n]$ is modeled as zero mean white Gaussian noise with variance $\sigma^2/2A^2$. This model assumes that the additive white Gaussian noise in (5), causes negligible change in the amplitude of the signal. The effect of noise is only manifested in phase of received signal in the form of additive phase noise $u[n]$. This additive Gaussian phase model is a good approximation at high signal-to-noise ratio [24]. The phase of the received signal using the approximation of (24) is given as

$$\angle r[n] = \phi[n,\alpha] + u[n] \quad \text{for } n = 0, 1, \ldots, NN_s - 1,$$

Substituting the excess phase of CPM signal from (4), the phase of the received signal becomes

$$\angle r[n] = 2\pi h\sum_{i=-\infty}^{m}\alpha_i q_{n-iN_s} + u[n]. \quad (25)$$

Now, the phase difference can be defined as

$$\Delta_n = \angle r[n+1] - \angle r[n] \quad \text{for } n = 0, 1, \ldots, NN_s - 2, \quad (26)$$

which can be represented as

$$\Delta_n = \omega_n h + \Omega_n, \quad (27)$$

where

$$\Omega_n = u[n+1] - u[n] \quad (28)$$

is the differential phase noise and

$$\omega_n = 2\pi\sum_{z=0}^{L-1}\Delta Q_{jz}\alpha_{z+m}, \quad (29)$$

with $m = \lfloor\frac{n}{Ns}\rfloor$ and $j = (n)_{N_s}$. Here we have used the matrix ΔQ containing difference of samples of the phase shaping function, with elements defined as

$$\Delta Q_{jz} = q_{[L-z-1]N_s+j+1} - q_{[L-z-1]N_s+j}. \quad (30)$$

The vector form of (27) becomes

$$\Delta = \boldsymbol{\omega}h + \Omega, \quad (31)$$

where Δ, $\boldsymbol{\omega}$ and Ω are $(NN_s - 1) \times 1$ column vectors with n-th elements defined as Δ_n, ω_n and Ω_n, respectively. The noise vector Ω is complex Gaussian with zero mean and the covariance matrix $\mathbf{C}_\Omega$ is given as

$$\boldsymbol{C}_{\boldsymbol{\Omega}} = \frac{\sigma^2}{2A^2}\begin{bmatrix} 2 & -1 & 0 & \ldots & 0 \\ -1 & 2 & -1 & \ldots & 0 \\ \vdots & \vdots & \vdots & \ddots & \vdots \\ 0 & \vdots & 0 & -1 & 2 \end{bmatrix}. \quad (32)$$

Since it is apparent that the approximate vector model of (31) is generalized linear in the unknown parameter h with colored Gaussian noise, we can use the Gauss-Markov Theorem to determine the best linear unbiased estimator (BLUE) given by

$$\hat{h}_{BLUE} = \frac{\boldsymbol{\omega}^T \mathbf{C}_{\Omega}^{-1} \Delta}{\boldsymbol{\omega}^T \mathbf{C}_{\Omega}^{-1} \boldsymbol{\omega}}, \tag{33}$$

with variance of $\hat{h}_{BLUE}$ given as

$$Var_{(\hat{h}_{BLUE})} = \frac{1}{\boldsymbol{\omega}^T \mathbf{C}_{\Omega}^{-1} \boldsymbol{\omega}}. \tag{34}$$

It should be noted that the variance of the BLUE estimator will approach (34) only at high SNR when the approximation in (24) becomes accurate.

IV. MCRLB

In this section, we derive the modified Cramer-Rao lower bound (MCRLB) [25] for modulation index of the partial response CPM signal in AWGN. The sampled complex envelope of the CPM signal can be expressed as

$$s[n] = \mu_n + j\nu_n, \tag{35}$$

where

$$\mu_n = \cos\left(2\pi h \sum_{i=-\infty}^{m} \alpha_i q_{n-iN_s}\right), \tag{36}$$

and

$$\nu_n = \sin\left(2\pi h \sum_{i=-\infty}^{m} \alpha_i q_{n-iN_s}\right) \tag{37}$$

are the real and imaginary parts of the CPM signal, respectively. Similarly the received signal is given as

$$r[n] = \tilde{x}_n + j\tilde{y}_n, \tag{38}$$

where $\tilde{x}_n$ and $\tilde{y}_n$ are the real and imaginary parts of the received signal, respectively.

From [26], the expression for log-likelihood function of joint probability density function of received signal is given as

$$\log f(\mathbf{r}, h) = -N \log(\pi\sigma^2) - \frac{1}{\sigma^2} \sum_{n=0}^{NN_s-1} \left[(\tilde{x_n} - \mu_n)^2 + (\tilde{y_n} - \nu_n)^2\right],$$

where $\mathbf{r}$ is the vector of samples of the received signal $r[n]$. For this likelihood function [21], [26] the Fisher information function

$$I_h = -\mathbb{E}\left\{\frac{\partial^2}{\partial h^2} \log f(\mathbf{r}, h)\right\} \tag{39}$$

can be computed as

$$I_h = \frac{2}{\sigma^2} \sum_{n=0}^{NN_s-1} \left[\left(\frac{\partial \mu_n}{\partial h}\right)^2 + \left(\frac{\partial \nu_n}{\partial h}\right)^2\right]. \tag{40}$$

Partial derivatives are computed with respect to the parameter h and are given as

$$(\partial \mu_n / \partial h) = -\left[2\pi \sum_{i=-\infty}^{m} \alpha_i q_{n-iN_s}\right] \sin(\beta) \tag{41}$$

and

$$(\partial \nu_n / \partial h) = \left[2\pi \sum_{i=-\infty}^{m} \alpha_i q_{n-iN_s}\right] \cos(\beta), \tag{42}$$

where $\beta = 2\pi h \sum_{i=-\infty}^{m} \alpha_i q_{n-iN_s}$.

Substituting the above values in (39), Fisher information becomes

$$I_h = \frac{2}{\sigma^2} \sum_{n=0}^{NN_s-1} \left[2\pi \sum_{i=-\infty}^{m} \alpha_i q_{n-iN_s}\right]^2. \tag{43}$$

Separating the cumulative and correlative components, we get

$$I_h = \frac{8\pi^2}{\sigma^2} \sum_{n=0}^{NN_s-1} \left[\frac{1}{2} \sum_{i=-\infty}^{m-L} \alpha_i + \sum_{i=m-L+1}^{m} \alpha_i q_{n-iN_s}\right]^2. \tag{44}$$

Expanding the square, we obtain

$$I_h = \frac{8\pi^2}{\sigma^2} \sum_{n=0}^{NN_s-1} \left[\left(\sum_{i=-\infty}^{m-L} \frac{\alpha_i}{2}\right)^2 + \left(\sum_{i=m-L+1}^{m} \alpha_i q_{n-iN_s}\right)^2 + \left(\sum_{i=0}^{m-L} \alpha_i\right)\left(\sum_{i=m-L+1}^{m} \alpha_i q_{n-iN_s}\right)\right]. \tag{45}$$

To evaluate the first term, i.e.,

$$\mathrm{I} = \sum_{n=0}^{NN_s-1} \left(\sum_{i=-\infty}^{m-L} \frac{\alpha_i}{2}\right)^2, \tag{46}$$

we split the term in parenthesis to get

$$\mathrm{I} = \frac{1}{4} \sum_{n=0}^{NN_s-1} \left[\sum_{i=-\infty}^{-L} \alpha_i + \sum_{i=-L+1}^{m-L} \alpha_i\right]^2. \tag{47}$$

For simplicity of notation, let $\gamma = \sum_{i=-\infty}^{-L} \alpha_i$. Using this definition in (47), we get

$$\begin{aligned} \mathrm{I} &= \frac{1}{4}\Big[N_s\gamma^2 + N_s(\gamma + \alpha_{-L+1})^2 \\ &\qquad + \ldots + N_s(\gamma + \ldots + \alpha_{N-L-1})^2\Big] \\ &= \frac{N_s}{4}\gamma^2 + \frac{N_s}{4} \sum_{m=1}^{N-1} \left[\gamma + \sum_{i=-L+1}^{m-L} \alpha_i\right]^2. \end{aligned} \tag{48}$$

Averaging the first term over the M-ary memoryless data symbols, we get

$$\bar{\mathrm{I}} = \frac{N_s}{4} \sum_{m=1}^{N-1} m\frac{(M^2-1)}{3} = \frac{N_s N(N-1)(M^2-1)}{24}. \tag{49}$$

Now evaluating the second term, i.e., $\sum_{n=0}^{NN_s-1}[\sum_{i=m-L+1}^{m}\alpha_i q_{n-iN_s}]^2$, we obtain

$$\begin{aligned}\mathrm{II} = \sum_{m=0}^{N-1}\Big[&(\alpha_m q_0 + \alpha_{m-1}q_{N_s} + .. + \alpha_{m-L}q_{(L-1)N_s})^2 + \ldots \\ &+ (\alpha_m q_j + \alpha_{m-1}q_{N_s+j} + \ldots + \alpha_{m-L}q_{(L-1)N_s+j})^2 + \ldots \\ &+ (\alpha_m q_{N_s-1} + \alpha_{m-1}q_{2N_s-1} + \ldots + \alpha_{m-L}q_{LN_s-1})^2\Big]\end{aligned} \tag{50}$$

Now, the expectation is applied over data symbols due to which cross terms disappear, as symbols are uncorrelated with zero mean. Eq (50) thus becomes

$$\begin{aligned}\bar{\mathrm{II}} &= \frac{M^2-1}{3}\Big[(q_0^2 + q_{N_s}^2 + .. + q_{(L-1)N_s}^2) \\ &\quad + (q_1^2 + q_{N_s+1}^2 + \ldots + q_{(L-1)N_s+1}^2)5 \\ &\quad + .. + (q_{N_s-1}^2 + q_{2N_s-1}^2 + \ldots + q_{LN_s-1}^2)\Big] \\ &= \frac{M^2-1}{3}\sum_{k=0}^{LN_s-1} q_k^2.\end{aligned} \tag{51}$$

Considering the third term, i.e.,

$$\mathrm{III} = \left(\sum_{i=0}^{m-L}\alpha_i\right)\left(\sum_{i=m-L+1}^{m}\alpha_i q_{n-iN_s}\right), \tag{52}$$

it is easy to observe that when averaged over the data sequence, it becomes

$$\bar{\mathrm{III}} = 0, \tag{53}$$

since symbols are mutually uncorrelated. Now, using (49), (51) and (53), the modified Fisher Information becomes

$$\bar{I}_h = \frac{8\pi^2 N(M^2-1)}{3\sigma^2}\left[\frac{N_s(N-1)}{8} + \sum_{k=0}^{LN_s-1} q_k^2\right], \tag{54}$$

which is a general expression for the modified Fisher information of partial response single-h CPM signals. Thus, the expression for the modified CRLB (MCRLB) can be obtained by inverting the modified Fisher information, i.e.,

$$\begin{aligned}\mathrm{MCRLB}_h &= \bar{I}_h^{-1} \\ \mathrm{MCRLB}_h &= \frac{3\sigma^2}{8\pi^2 N(M^2-1)}\left[\frac{N_s(N-1)}{8} + \sum_{k=0}^{LN_s-1} q_k^2\right]^{-1}.\end{aligned} \tag{55}$$

For example, for a binary CPM scheme with rectangular phase shaping function, $q_k = \frac{k}{2LN_s}$, and the expression of MCRLB becomes

$$\mathrm{MCRLB}_h = \frac{\sigma^2}{\pi^2 N}\left[\frac{3LN_s}{3LN_s^2(N-1)+(LN_s-1)(2LN_s-1)}\right]. \tag{56}$$

It can be observed from the final expression of MCRLB that it does not depend upon the parameter of interest, i.e., the modulation index h. The MCRLB depends on the number of samples per symbol N_s, number of symbols N, variance σ^2 and the phase shaping function q_k. It is also interesting to note that the dependence on N is stronger than on N_s and for large N, the dependence on the partial response length L becomes negligible.

V. NUMERICAL RESULTS

In this section, we report the results of numerical simulations to study and assess the performance of the proposed estimators in Section III-A and Section III-B with reference to the MCRLB in Section IV. We also compare the MSE performance of the proposed estimators with existing estimators for the partial response modulation schemes. Specifically, we compare the proposed data-aided BLUE estimator with DA-LNDIF [14] and the proposed non-data aided MoM estimator with NDA-CYC [12]. The numerical simulations have been performed in MATLAB. Unless mentioned otherwise, we consider binary partial response CPM schemes with rectangular phase shaping functions. The channel model assumed is AWGN with varying noise power. The MSE reported in the results is obtained by averaging over 1000 Monte Carlo trials.

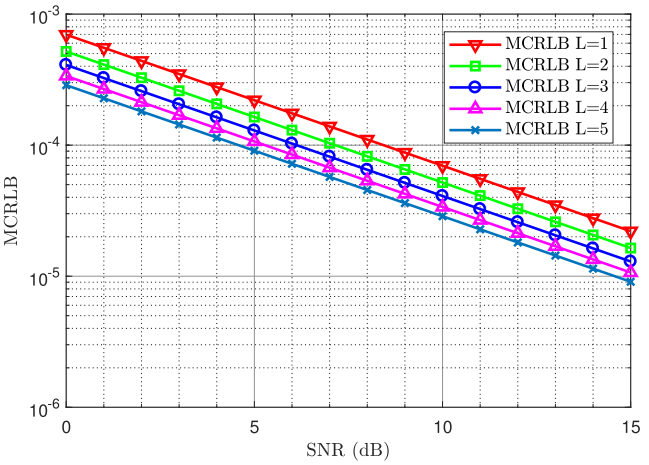

FIGURE 1. MCRLB of CPM vs. SNR for five different values of partial response length with $N_s = 4$, $N = 5$.

In Fig. 1, the MCRLB of CPM is plotted against the SNR for increasing values of partial response length L with $Ns = 4$, $N = 5$ and $h = 0.5$. It is clear from the figure that MCRLB decreases with the increase in SNR as noise power reduces. It can also be observed that MCRLB is also slightly reduced by increasing the values of L. However, for larger values of N, the decrease in MCRLB becomes negligible. Hence, theoretically, the performance of efficient estimators for increasing partial response length L may not deteriorate at all. However, we will see later that for both the data-aided and non-data aided estimators of [12] and [14], respectively, the performance severely degrades with increase in the partial response length L.

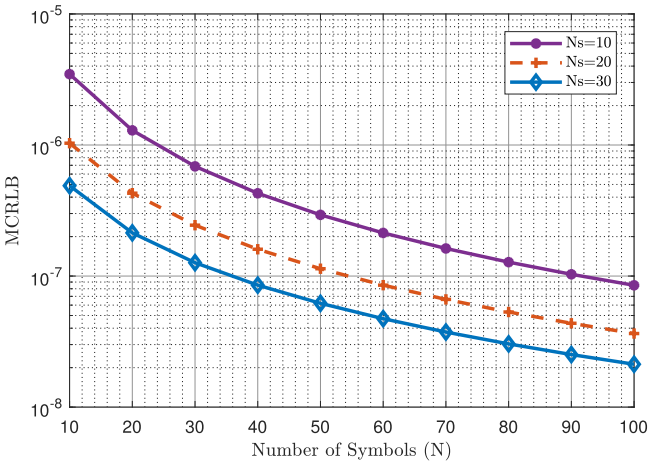

FIGURE 2. MCRLB of CPM vs. N for three different values of N_S with SNR = 10dB, $L = 3$ and $h = 0.5$.

Fig. 2 illustrates the dependence of MCRLB of partial response CPM on N for different values of N_s with fixed values $L = 3$ and SNR = 10dB. We can observe that MCRLB decays when either N or N_s is increased. As indicated by (56), and also verified by simulations, the MCRLB decays faster with increasing number of symbols N as compared to the decrease with increasing samples per symbol N_s. Similar effect is obtained for other values of partial response length L and and SNRs.

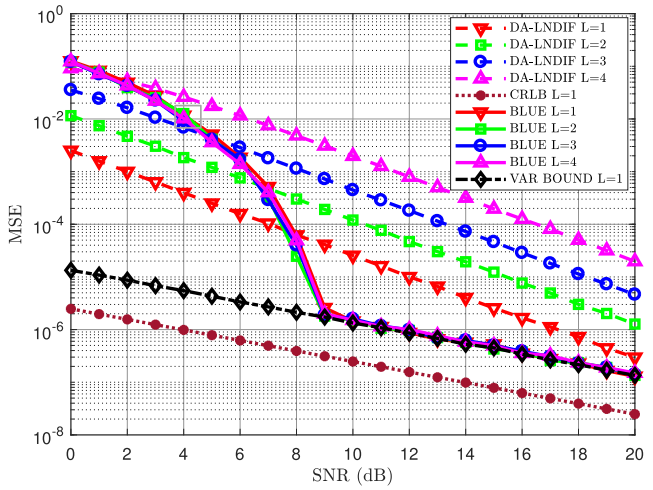

FIGURE 3. MSE of DA-LNDIF and BLUE estimators, compared with MCRLB vs.SNR with $N = 100$, $N_S = 4$ and $h = 0.5$.

Fig. 3 provides the performance comparison of data-aided BLUE estimator (see (33)) with DA-LNDIF estimator [14] with reference to the MCRLB. The simulations are performed at $N = 100$, $N_s = 4$ and $h = 0.5$. The MCRLB and variance bound for linear estimators of Eq. (34) are plotted only for $L = 1$ for the sake of simplicity in the figure. The MCRLB and variance bound for $L > 1$ is almost equal to that of $L = 1$ since the dependence of MCRLB on the value of L is very weak for values of $N > 50$ (see (56)). We can observe that the DA-LNDIF estimator has better performance at low SNR. Our proposed BLUE estimator has better performance than DA-LNDIF at high SNR and gets close to the MCRLB and achieves the variance bound for linear estimators. At low SNR, the additive phase noise approximation of (24) is not very accurate thus leading to the inferior performance in this region. The approximate linear model (24) used for BLUE is accurate for high SNR scenarios. It can be observed that the performance of BLUE estimator is preserved for different partial response lengths. On the contrary, the performance of DA-LNDIF worsens when L increases. DA-LNDIF considers only the principle component of CPM signal but when L increases, the energy is contained not only in the principal component but also spread in other components of Laurent's pulses. Thus the performance of DA-LNDIF degrades when partial response length L increases. The MSE of the BLUE estimator, the MCRLB and the variance bound show very similar trend for the raised cosine phase shaping function.

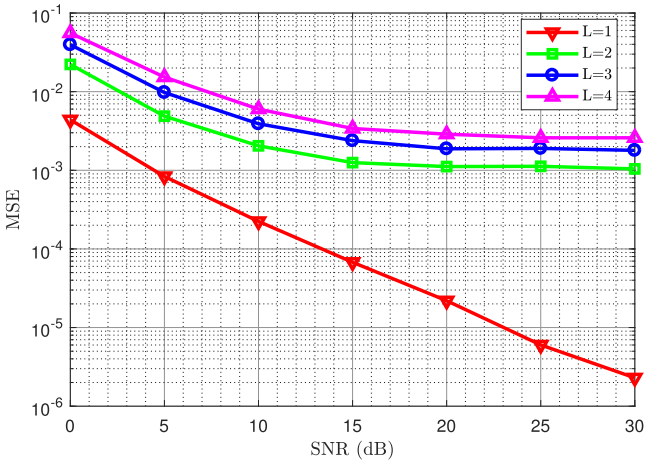

FIGURE 4. MSE of method of moments estimator vs. SNR for different partial response lengths with $N = 100$ and $h = 0.5$.

Fig. 4 presents the performance of the non-data aided MoM estimator of (23). Figure shows the dependence of MSE of MoM estimator on the value of L and SNR at fixed values of $N = 100$ and $h = 0.5$. It can be observed that the performance of estimator improves with the SNR. However, the MSE deteriorates with increase in the memory of the modulation scheme, i.e., for larger values of L.

Fig. 5 shows the MSE of MoM estimator plotted against number of data symbols N for three different values of SNR. The parameters fixed for the simulation are $L = 3$ and $h = 0.5$. It is clear from the figure that the performance of estimator improves when SNR is increased but the gains with SNR are diminishing, as is true for most non-data aided estimators. Also, MSE improves for increasing number of data symbols N.

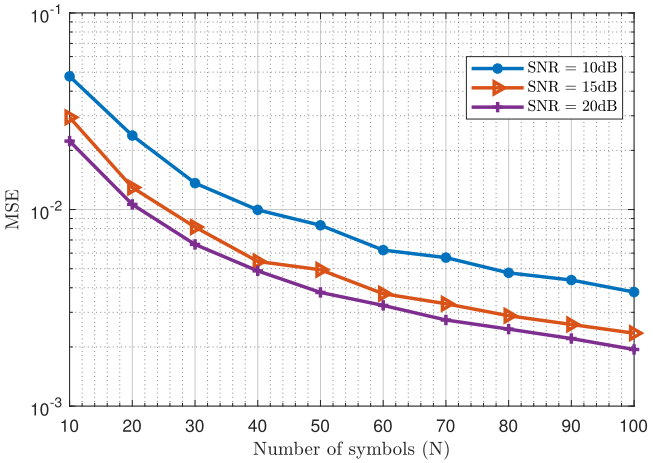

FIGURE 5. MSE of method of moments estimator vs. N for three different values of SNR with $L = 3$ and $h = 0.5$.

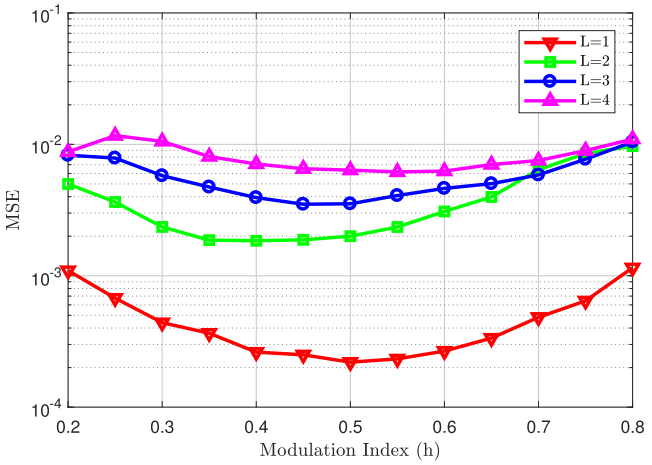

FIGURE 7. MSE of method of moments estimator vs. h for SNR = 10dB and $N = 100$.

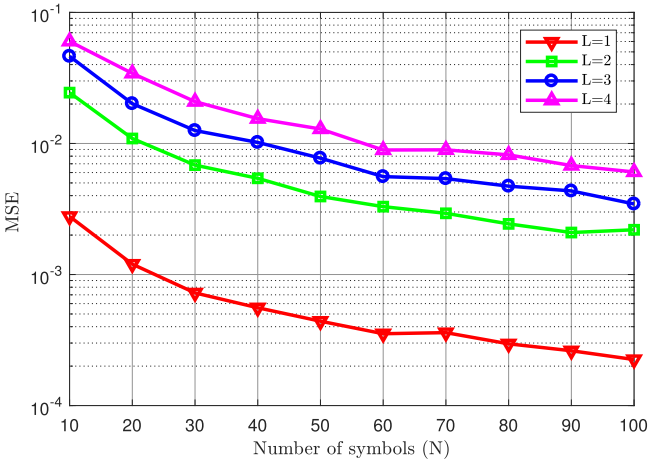

FIGURE 6. MSE of method of moments estimator vs. N for different partial response lengths with SNR = 10dB and $h = 0.5$.

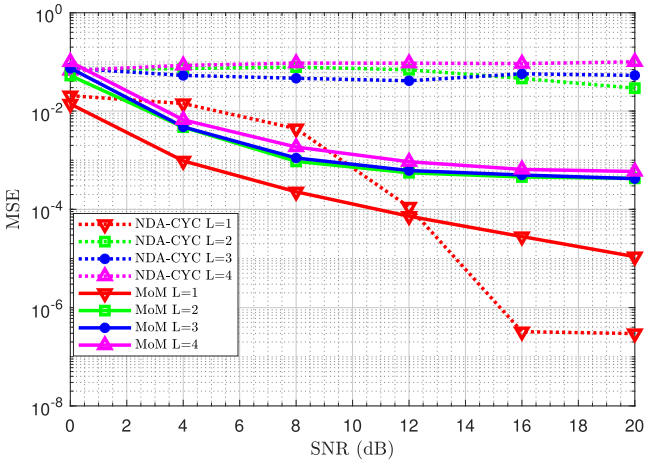

FIGURE 8. MSE of NDA-CYC and MoM estimators vs. SNR with $N = 1000$, $N_s = 1$ and $h = 0.7$.

In Fig. 6, we show the MSE of MoM estimator plotted against number of data symbols N. The simulations are performed for $h = 0.5$ and SNR = 10 dB. The performance of the estimator strongly depends upon the number of available symbols N, as it can be observed that MSE decreases with the increase in N. As observed earlier, the MSE of MoM estimator deteriorates for larger values of L.

In Fig. 7, we report the results of MSE of the proposed MoM estimator vs. parameter h for different values of L. The parameters fixed for the simulation are SNR = 10dB and $N = 100$. Again, the performance of MoM estimator is better at lower values of L. The MSE shows some dependence upon the value of the modulation index h. It decreases initially with the increase in h with lowest values around $h = 0.5$, but is particularly high for values of h close to either 0 or 1. The behavior of the MSE is similar to the minimum distance of the CPM schemes [1].

Fig. 8 depicts the comparison of MSE vs. SNR of non-data aided MoM estimator with NDA-CYC estimator proposed in [12]. The simulations are performed over fixed parameters of $N = 1000$ symbols, $h = 0.7$ and $N_s = 1$. The simulation parameters have been chosen to get comparable results to those of [12]. It can be observed that MoM estimator performs well at low SNR for all values of L. The poor performance of NDA-CYC at low SNR is due to phase unwrapping errors as already identified in [14]. However, NDA-CYC estimator has better performance at high SNR for $L = 1$, but as partial response length L increases, its performance deteriorates even at high SNR.

In Fig. 9, performance of BLUE estimator is analyzed for $M = 4$ and compared with the binary case, i.e., $M = 2$. The simulations are performed for $L = 2$ by taking fixed values of $N = 100$ symbols, $N_s = 4$ and $h = 0.5$. It is clear from the figure that the performance is improved for $M = 4$ as MSE gets better, while the MCRLB and variance bound are also reduced.

For the data-aided case, the proposed BLUE estimator shows very good performance that approaches the linear

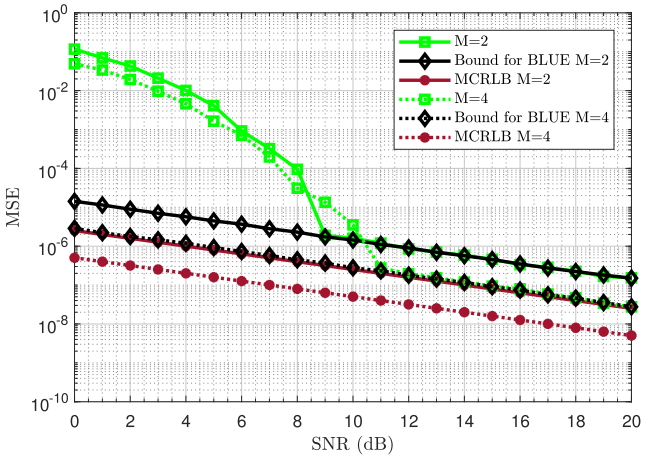

FIGURE 9. MSE of BLUE estimator vs. SNR for $M = 2$ and $M = 4$ with $L = 2$, $N = 100$, $N_s = 4$ and $h = 0.5$.

variance bound of (34) and becomes close to the MCRLB at high SNR. Moreover, its performance is not degrading with increasing partial response length when compared with DA-LNDIF [14], MoM and NDA-CYC. The proposed MoM estimator though shows better preservation of performance with respect to partial response length when compared with NDA-CYC [12], but still the performance loss is considerable. Another advantage of the proposed MoM estimator over the previously proposed NDA-CYC is its non-iterative nature and low computational complexity. In the future, we intend to further explore the concept of non-data aided modulation index estimation for general phase shaping functions and work towards improving the MSE performance for CPM schemes with large partial response memory. Another future direction could be the asymptotic performance analysis of the proposed MoM estimator using statistical linearization approach.

VI. CONCLUSIONS

In this paper, we have proposed two novel estimators and derived the modified Cramer Rao lower bound (MCRLB) for the modulation index estimation of partial response CPM signals. The MCRLB expression is independent of the modulation index itself but shows a weak dependence on the partial response length. The data aided BLUE estimator performs very well at high SNR, approaches close to the MCRLB and shows robust performance against increasing modulation memory. The MoM estimator is non-iterative and shows superior performance at low SNR as compared to the existing non-data aided approaches.

APPENDIX

In this appendix, we discuss the derivation of fourth-order cumulants in equations (20) and (21) using the auto-correlation function for the partial response CPM schemes in (19). Using the definition of cumulants function in (7) at $m_1 = 0$, $m_2 = 0$ and $m_3 = 0$, we get

$$\begin{aligned} c(0,0,0) &= \mathbb{E}\{s^*[n]s[n]s[n]s^*[n]\} \\ &\quad - \mathbb{E}\{s^*[n]s[n]\}\mathbb{E}\{s[n]s^*[n]\} \\ &\quad - \mathbb{E}\{s^*[n]s[n]\}\mathbb{E}\{s[n]s^*[n]\} \\ &\quad - \mathbb{E}\{s^*[n]s^*[n]\}\mathbb{E}\{s[n]s[n]\}, \end{aligned} \tag{57}$$

which can be expressed as

$$\begin{aligned} c(0,0,0) &= \mathbb{E}\{|s[n]|^2\,|s[n]|^2\} - R^2\,[0] - R^2\,[0] \\ &\quad - \mathbb{E}\{s^*[n]s^*[n]\}\mathbb{E}\{s[n]s[n]\}, \end{aligned} \tag{58}$$

where

$$R[0] = A^2 \tag{59}$$

is the mean-squared value of the CPM signal and

$$|s[n]|^2 = Ae^{j\phi[n,\alpha]}Ae^{-j\phi[n,\alpha]} = A^2. \tag{60}$$

While the last term in (58) can be shown to be equal to zero as follows:

$$\begin{aligned} &\mathbb{E}\{s^*[n]s^*[n]\}\mathbb{E}\{s[n]s[n]\} \\ &= \mathbb{E}\{A^2\,e^{-j2\phi[n,\alpha]}\}\mathbb{E}\{A^2\,e^{j2\phi[n,\alpha]}\} \\ &= A^4\mathbb{E}\{e^{-j2\pi h\sum_{i=-\infty}^{n-L}\alpha_i}.e^{-j4\pi h\sum_{i=0}^{L-1}\alpha_{n-i}q_i}\}. \\ &\quad \mathbb{E}\{e^{j2\pi h\sum_{i=-\infty}^{n-L}\alpha_i}.e^{j4\pi h\sum_{i=0}^{L-1}\alpha_{n-i}q_i}\} \\ &= \mathbb{E}\{Ae^{-j2\pi h\sum_{i=-\infty}^{n-L}\alpha_i}\}.\mathbb{E}\{e^{-j4\pi h\sum_{i=0}^{L-1}\alpha_{n-i}q_i}\}. \\ &\quad \mathbb{E}\{Ae^{j2\pi h\sum_{i=-\infty}^{n-L}\alpha_i}\}.\mathbb{E}\{e^{j4\pi h\sum_{i=0}^{L-1}\alpha_{n-i}q_i}\} \\ &= 0 \end{aligned} \tag{61}$$

The last term is zero as the expectation of $\mathbb{E}\{e^{j2\theta_{n-L}}\} = 0$ is zero over the cumulative phase $\theta_{n-L} := \pi h\sum_{i=-\infty}^{n-L}\alpha_i$ taking values $\theta_{n-L} \in \{0, \frac{2\pi}{p}, \frac{4\pi}{p}, \ldots, \frac{2(p-1)\pi}{p}\}$, where p is an integer such that $h = \frac{2l}{p}$ for an integer l. Thus, combining (59), (60) and (61), we get

$$c(0,0,0) = -A^4 \tag{62}$$

Similarly, using the definition of cumulants function in (7) at $m_1 = 0$, $m_2 = 0$ and $m_3 = 1$, we get

$$\begin{aligned} c(0,0,1) &= \mathbb{E}\{s^*[n]s[n]s[n]s^*[n+1]\} \\ &\quad - \mathbb{E}\{s^*[n]s[n]\}\mathbb{E}\{s[n]s^*[n+1]\} \\ &\quad - \mathbb{E}\{s^*[n]s[n]\}\mathbb{E}\{s[n]s^*[n+1]\} \\ &\quad - \mathbb{E}\{s^*[n]s^*[n+1]\}\mathbb{E}\{s[n]s[n]\}, \end{aligned} \tag{63}$$

where

$$s[n+1] = Ae^{j\pi h\sum_{i=-\infty}^{n-L+1}a_i}.e^{j2\pi h\sum_{i=0}^{L-1}a_{n-i+1}q_i}, \tag{64}$$

Simplifying each term of (63) separately, we get

$$\begin{aligned} \mathrm{I}_1 &= \mathbb{E}\{s^*[n]s[n]s[n]s^*[n+1]\} \\ &= \mathbb{E}\{|s[n]|^2 s[n]s^*[n+1]\} \\ &= A^2\mathbb{E}\{s[n]s^*[n+1]\} \\ &= A^2.R[-1] \end{aligned} \tag{65}$$

As autocorrelation is an even function, thus $R[-1] = R[1]$ and using (19) we obtain

$$\mathrm{I}_1 = A^4 \cos^L\left(\frac{\pi h}{L}\right). \tag{67}$$

Similarly, the second term of (63) can be simplified as

$$\begin{aligned}\mathrm{II}_1 &= \mathbb{E}\{s^*[n]s[n]\}\mathbb{E}\{s[n]s^*[n+1]\} \\ &= A^2 R[-1] \\ &= A^2 R[1] \\ &= A^4 \cos^L\left(\frac{\pi h}{L}\right)\end{aligned} \tag{68}$$

Third term is identical to second term, i.e.,

$$\mathrm{III}_1 = A^4 \cos^L\left(\frac{\pi h}{L}\right). \tag{69}$$

Now, the fourth term of (63) can be shown as zero as follows:

$$\begin{aligned}\mathrm{IV}_1 &= \mathbb{E}\{s^*[n]s^*[n+1]\}\mathbb{E}\{s[n]s[n]\} \\ &= 0,\end{aligned} \tag{70}$$

Since the second factor $\mathbb{E}\{s[n]s[n]\} = 0$ using the same justification as in (61). Thus,

$$c(0,0,1) = -A^4 \cos^L\left(\frac{\pi h}{L}\right). \tag{71}$$

This establishes equations (20) and (21) in Section III-A.

REFERENCES

[1] C. E. Sundberg, "Continuous phase modulation," *IEEE Commun. Mag.*, vol. 24, no. 4, pp. 25–38, Apr. 1986.
[2] F. Xiong, F. Xiong, and F. Xiong, *Digital Modulation Techniques*, vol. 633. Boston, MA, USA: Artech House, 2000.
[3] K. Murota and K. Hirade, "GMSK modulation for digital mobile radio telephony," *IEEE Trans. Commun.*, vol. COM-29, no. 7, pp. 1044–1050, Jul. 1981.
[4] *ESTI, Digital Enhanced Cordless Telecommunications (DECT); Ultra Low Energy (ULE); Machine to Machine Communications; Part 1: Home Automation Network (Phase 1)*, Standard ETSI TS 102 939-1, ETSI, Sophia Antipolis, France, 2013.
[5] *Bluetooth Standard Core Version*, B.S.I.G. (SIG), Bluetooth SIG Inc., Kirkland, WA, USA, 2010.
[6] D. Bonacci, R. Prévost, J.-P. Millerioux, J. LeMaitre, M. Coulon, and J.-Y. Tourneret, "Advanced concepts for satellite reception of AIS messages," in *Proc. Toulouse Space Show*, 2012, pp. 25–28.
[7] G. K. Kaleh, "Simple coherent receivers for partial response continuous phase modulation," *IEEE J. Sel. Areas Commun.*, vol. 7, no. 9, pp. 1427–1436, Dec. 1989.
[8] M. Messai, G. Colavolpe, K. Amis, and F. Guilloud, "Binary continuous phase modulations robust to a modulation index mismatch," *IEEE Trans. Commun.*, vol. 63, no. 11, pp. 4267–4275, Nov. 2015.
[9] M. Messai, G. Colavolpe, K. Amis, and F. Guilloud, "Robust detection of binary CPMs with unknown modulation index," *IEEE Commun. Lett.*, vol. 19, no. 3, pp. 339–342, Mar. 2015.
[10] U. Mengali and M. Morelli, "Decomposition of M-ary CPM signals into PAM waveforms," *IEEE Trans. Inf. Theory*, vol. 41, no. 5, pp. 1265–1275, Sep. 1995.
[11] J. R. Fonollosa and J. A. R. Fonollosa, "Estimation of the modulation index of CPM signals using higher-order statistics," in *Proc. IEEE Int. Conf. Acoust., Speech, Signal Process. (ICASSP)*, vol. 4. Apr. 1993, pp. 268–271.
[12] P. Bianchi, P. Loubaton, and F. Sirven, "Non data-aided estimation of the modulation index of continuous phase modulations," *IEEE Trans. Signal Process.*, vol. 52, no. 10, pp. 2847–2861, Oct. 2004.
[13] P. Bianchi, P. Loubaton, and F. Sirven, "On the blind estimation of the parameters of continuous phase modulated signals," *IEEE J. Sel. Areas Commun.*, vol. 23, no. 5, pp. 944–962, May 2005.
[14] D. Xu and Y. Zhang, "Estimation of the modulation index of CPM signals based on Laurent's decomposition," *IEEE Trans. Wireless Commun.*, vol. 12, no. 12, pp. 6268–6280, Dec. 2013.
[15] M. Messai, F. Guilloud, and K. Amis, "A low complexity coherent CPM receiver with modulation index estimation," in *Proc. 22nd Eur. Signal Process. Conf. (EUSIPCO)*, Sep. 2014, pp. 979–983.
[16] A. Napolitano and C. M. Spooner, "Cyclic spectral analysis of continuous-phase modulated signals," *IEEE Trans. Signal Process.*, vol. 49, no. 1, pp. 30–44, Jan. 2001.
[17] P. Laurent, "Exact and approximate construction of digital phase modulations by superposition of amplitude modulated pulses (AMP)," *IEEE Trans. Commun.*, vol. COM-34, no. 2, pp. 150–160, Feb. 1986.
[18] T. Nelson, E. Perrins, and M. Rice, "Near optimal common detection techniques for shaped offset QPSK and Feher's QPSK," *IEEE Trans. Commun.*, vol. 56, no. 5, pp. 724–735, May 2008.
[19] S. Tretter, "Estimating the frequency of a noisy sinusoid by linear regression (Corresp.)," *IEEE Trans. Inf. Theory*, vol. IT-31, no. 6, pp. 832–835, Nov. 1985.
[20] S. Kay, "A fast and accurate single frequency estimator," *IEEE Trans. Acoust., Speech Signal Process.*, vol. 37, no. 12, pp. 1987–1990, Dec. 1989.
[21] S. M. Kay, *Fundamentals of Statistical Processing: Estimation Theory*, vol. 1. Englewood Cliffs, NJ, USA: Prentice Hall, 1993.
[22] J. R. Fonollosa and C. L. Nikias, "Analysis of CPM signals using higher-order statistics," in *Proc. Conf. Rec. Commun. Move IEEE Military Commun. Conf. (MILCOM)*, vol. 2. Oct. 1993, pp. 663–667.
[23] G. Cariolaro and A. M. Cipriano, "Minimal PAM decompositions of CPM signals with separable phase," *IEEE Trans. Commun.*, vol. 53, no. 12, pp. 2011–2014, Dec. 2005.
[24] H. Fu and P.-Y. Kam, "Phase-based, time-domain estimation of the frequency and phase of a single sinusoid in AWGN—The role and applications of the additive observation phase noise model," *IEEE Trans. Inf. Theory*, vol. 59, no. 5, pp. 3175–3188, May 2013.
[25] A. N. D'Andrea, U. Mengali, and R. Reggiannini, "The modified Cramer-Rao bound and its application to synchronization problems," *IEEE Trans. Commun.*, vol. 42, no. 234, pp. 1391–1399, Feb./Apr. 1994.
[26] S. Peleg and B. Porat, "The Cramer-Rao lower bound for signals with constant amplitude and polynomial phase," *IEEE Trans. Signal Process.*, vol. 39, no. 3, pp. 749–752, Mar. 1991.

TAYYABA MUNAWAR received the B.E. degree in electrical engineering from the University of Engineering and Technology, Peshawar, Pakistan, in 2014, and the M.S. degree in electrical engineering from the National University of Sciences and Technology, Islamabad, Pakistan, in 2018. Her research interests include signal processing for communication with a focus on detection and estimation theory.

SAJID SALEEM (S'09–M'14) received the B.Sc. degree in electrical engineering from the National University of Sciences and Technology, Islamabad, Pakistan, in 2006, the M.S. degree in mathematics and the Ph.D. degree in electrical and computer engineering from the Georgia Institute of Technology, Atlanta, GA, USA, in 2011 and 2013, respectively. Since 2014, he has been an Assistant Professor with the School of Electrical Engineering and Computer Science, National University of Sciences and Technology. His research interests include signal processing for biomedical engineering and communications, brain-computer interfaces, and time-frequency analysis.

SYED ALI HASSAN (S'07–M'12–SM'17) received the B.E. degree (Hons.) in electrical engineering from the National University of Sciences and Technology (NUST), Pakistan, in 2004, the M.S. degree in electrical engineering from the University of Stuttgart, Germany, in 2007, the M.S. degree in mathematics from the Georgia Institute of Technology (Georgia Tech), Atlanta, USA, in 2011, and the Ph.D. degree in electrical engineering from Georgia Tech in 2011. His research interests include signal processing for communications. He is currently an Assistant Professor with the School of Electrical Engineering and Computer Science (SEECS), NUST, where he is the Director of Information Processing and Transmission Research Group, which focuses on various aspects of theoretical communications. Prior to joining SEECS, he was a Research Associate with Cisco Systems Inc., San José, CA, USA. He has co-authored over 100 publications in international conferences and journals. He served as a TPC Member for the IEEE WCSP 2014, the IEEE PIMRC 2013–2014, the IEEE VTC Spring 2013–2017, and the MILCOM 2014-2017, among others.

SYED MOHAMMAD HASSAN ZAIDI received the B.S. degree in aviation electronics from the College of Aeronautical Engineering, Pakistan, in 1984, and the M.S. degree in electrical engineering and the Ph.D. degree from the University of South Florida, Tampa, Fl, USA, in 1989 and 1992, respectively. He is currently the Principal and the Dean of School of Electrical Engineering and Computer Science, National University of Sciences and Technology, Islamabad, Pakistan. His research interests include high-speed multichannel optical communication, signal processing, and wireless sensor networks. He was a recipient of several coveted honors and awards, which notably include the NCR National IT Excellence Award for Research and Development.